Plasmonics
https://doi.org/10.1007/s11468-021-01405-w

Multi-layer MoS_2-Based Plasmonic Gold Nanowires at Near-Perfect Absorption for Energy Harvesting

Zakariae Oumekloul[1,3] · Shuwen Zeng[2] · Younes Achaoui[1] · Abdellah Mir[1] · Abdellatif Akjouj[3]

Received: 9 September 2020 / Accepted: 11 February 2021

Abstract
One of the biggest challenges in relation to the modernistic vision of smart city technology is to provide confident autonomous energy, notably in terms of power storage. If you want to change an existing lifestyle, you cannot ignore the basic concepts collected from basic physics. The subject of Metamaterials stands for an important research area that can be explored and used to come up with unparalleled ideas about the properties and functions that are completely absent from natural materials. In contrast to other bold technologies, combining a simple layered surface with appropriate material selection makes it possible to pattern and manufacture new types of solar cells that work in a wide frequency range. In this article, we propose a simple method to boost the coupling interaction between metallic gold nanowires with multiple MoS_2 layers. The innovation of this work is that the thickness layer changes have great stability in the influence of the absorption performance and electric field distribution in the visible light and near-infrared spectra. Therefore, this new design can be seen as very important in many fields from sensing to solar cell applications.

Keywords Localized surface plasmon resonance · Gold nanowires · 2D materials · Transition metal dichalcogenides

Introduction

Surface plasmons (SPs), induced from collective oscillations of free electrons in the conduction band of metals, are some kind of vanishing waves that are delicate to changes in optical properties in the surrounding medium. It is notorious for the fact that p-polarization will cause charges to be generated at the metal interface and excite SP. This phenomenon occurs when the necessary momentum of incident light is provided through a prism [1] and is commonly referred to as surface plasmon resonance (SPR). Under these specific conditions, the maximum energy of TM polarized light is transferred to the electrons and produces a sharp peak in the absorption spectrum. This evidence provides the concept of a plasma absorber designed based on metal nanostructures. Nowadays, the system is assigned as a basis for integration into next-generation solar cells to aim smart energy–collecting devices.

Localized surface plasmon resonance (LSPR) is a type of SP related to metal particles whose size is much smaller than the radiation wavelength. The aforementioned basic physics of LSPR has opened up a new way to design metal nanostructures, which has aroused great interest in potential current and future applications. From then on, plasma absorbers have been developed rapidly, and various applications have been found, including biosensors [2–9], dedicated to proteins[10] and the label-free detection of antibodies [11, 12], photoelectric devices [13, 14], to improve the efficiency of photovoltaic cells [15]. In addition, the study of many physical parameters of nanostructures makes it a hopeful promising evaluation for the next generation of fascinating surfaces. Numerical models can be used to optimize and evaluate parameters such as the chemical composition of the substrate on which the metal is deposited, the size and form of the particles, and the surrounding environment to predict its effects. In addition,

✉ Zakariae Oumekloul
z.oumekloul@edu.umi.ac.ma

[1] Laboratory for the Study of Advanced Materials and Applications (LEM2A), Physics Department, Moulay Ismail University of Meknes, B.P. 11201, Meknes, Zitoune, Morocco

[2] XLIM Research Institute, UMR 7252 CNRS, University of Limoges, 123 Avenue Albert Thomas, Limoges, France

[3] Department of Physics, Institute of Electronics, Microelectronics and Nanotechnology, CNRS-8520, FST, University of Lille, 59652 Villeneuve d'Ascq, France

Published online: 20 March 2021

these models allow the development of new materials such as graphene and 2D transition dichalcogenide (TMDs) as molybdenum disulfide (MoS_2) and tungsten disulfide (WS_2) [10, 16, 17].

The interaction between nanoparticles and 2D materials (such as MoS_2) provides further outlooks for optoelectronic applications. In the sub-nanometer distance, due to the tunneling effect of electrons between the metal nanoparticles and the active semiconductor layer, other functions also play a role. MoS_2 is a two-dimensional nanomaterial containing a hexagonal crystal lattice, in which atoms bind together by a strong linking of force and layer composite by van der Waals forces. From a plasmon perspective, compared with other materials, MoS_2 has supporting optical and tribological properties. First, concerning electron distribution, MoS_2 has tribological properties including an almost zero friction or super-lubrication state. Secondly, MoS_2 has higher thermal stability and oxidation resistance. Finally yet importantly, nanoscale MoS_2 has a very elevated density, small size, large specific surface area, and a high specific surface energy.

Recently, many studies [18, 19] [20, p. 2] [21, 22] have been conducted to show that the integration of these monoatomic coating above the substrate allows a significant enhancement of the optical properties such as absorption [23], light emission [24], and photoluminescence [25]. However, studies on interactions using multi-layer TMDs have rarely been reported in the literature. Additionally, unlike the systems found in the literature, the simplicity of the design makes it easy to reduce difficulties for experimental realizations and with large absorption factors.

In this work, we report on a numerical study using the finite element method (FEM) and the Drude-Lorentz model to predict accurately the optical signature of a gold nanowire anchored onto MoS_2 surfaces. A particular attention is given to the influence of MoS_2 on the performances. By studying several MoS_2 thickness parameters, we highlighted the optimum configuration trade off; maximum absorption versus frequency range of operation.

This paper is structured as follows: in "Structure and Modeling Method," the structure and the modeling method used in this study are presented in detail. In "Results and Discussion," we address the results and discussions around several parameters and the design performances. The conclusion is given in "Conclusions."

Structure and Modeling Method

The numerical results are implemented by using the finite element method (FEM) with the COMSOL Multiphysics software. Our calculations were undertaken in a 2D model (along the *x*- and *y*-axes) by considering the propagation along the *y*-axis. The two boundaries (where the incident wave is defined and collected) correspond to port boundary conditions. This system of boundary conditions makes it possible to determine the elements of the S-matrix and thus to deduce therefrom the transmission, reflection, and absorption coefficients.

We applied the periodic boundary condition along the *x*-direction to simulate an infinite unit cell (see Fig. 1), and the structure is set to be with infinite size in the *z*-direction. The modeling space is discretized using a triangular mesh. The minimum mesh size inside the MoS_2 is equal to 0.1 nm. The input optical field, with a polarization direction of the transverse magnetic (TM) mode, is excited at the top part of the unit cell by a light source along the *y*-axis. The transmission spectra of the optical signal, detected at the bottom side of the unit cell, are collected in terms of the optical frequency. The absorption of the proposed structure can be given as follows: $A = 1\text{-}R\text{-}T$, where R and T are the reflection and transmission spectra of the proposed structure. All the absorption spectra are normalized with respect to the problem.

The plasmonic nanostructures investigated in this work are assembled with Au nanowires in hexagonal shapes. This hexagonal Au nanowire array designed here is configured by the height of H, the two diameter parameters of l and L, and where p is for the period pitch (see Fig. 1). This hexagonal nanowire periodic structure is arranged upon a N layer of

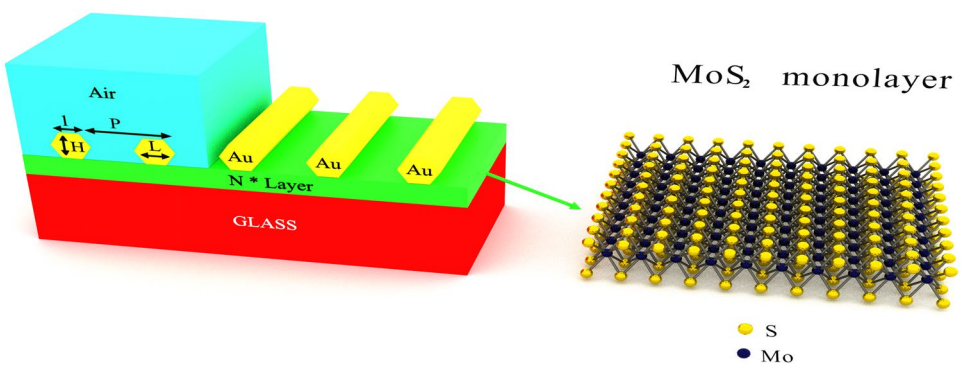

Fig. 1 3D sketch of MoS_2-based nanostructure

MoS_2 ($d_{MoS2} = N^*d = N^*0.646$ nm). The thickness of the monolayer MoS_2 has been previously measured experimentally by Li et al. [26]. The dispersion of MoS_2 was retrieved from the transmission measurements using a multi-Lorentzian model [26]. The absorption bands were represented by multiple resonances as:

$$\varepsilon(E) = \varepsilon_B + \sum_{j=0}^{N} \frac{f_j}{E_{0j}^2 - E^2 + iE\Gamma_j},$$

E represents the photon energy in eV, where ε_B, f_j, E_{0j} and Γ_j are respectively the non-resonant background dielectric permittivity, oscillator strength, resonance center energy, and the phenomenological damping constant of the absorption band j. All these parameters were varied to fit to experimental measurements. All details regarding the fitting process applied to the visible spectra were extracted from reference [27]. The parameter values are given in Table 1.

Finally, the MoS_2 was formed on a glass surface whose refractive index is estimated at 1.5 (Fig. 1). In the first part of this study, we have employed a light source with a normal incident angle as the excitation fields. After that, we changed the wavelength across the visible range in order to collect the localized SPR spectra of the metallic structures by optimizing both the periodicity and thickness of the TMD material.

The dielectric constant of gold nanoparticle is described by the Lorentz-Drude model. In the complex permittivity frequency-dependent analysis of metals [28], this model will allow us to fit experimental measurement data for the optical frequency-dependent dielectric parameters of metals with real and imaginary parts, in a relatively high precision in the visible range ($350 < \lambda < 900$ nm).

Results and Discussion

In order to maintain the shape of the designed hexagonal structure, the parameter L in these configurations should be larger than the value of parameter l. For the sake of simplicity, we have chosen $L = l + 10$ nm in the modeling. These geometrical parameters of the hexagonal nanowires are defined according to the experimental and numerical data in the literature [29], so the optimized parameters are: $l = 30$ nm, $L = 40$ nm, and $H = 15$ nm. Firstly, we evidenced strong absorption enhancement of MoS_2-based hexagonal gold nanostructure by means of plasmonic gold (Au) nanorods. Figure 1 shows the schematic structure consisted of 2D MoS_2 layers and gold nanowires. Through an appropriate design of gold nanowires displaying an LSPR frequency near the direct band gap of MoS_2 (1.86 eV), the localized SPR generated by the presence of Au nanowires will spectrally and spatially be coupled to the emission of the MoS_2 layers. And this strong coupling effect will result in a large enhancement at the optical absorption. Therefore, the geometrical parameters of gold nanowires have to be optimized to perform substantial absorption.

Table 1 The MoS_2 dispersion parameter values (see Ref. [27])

Oscillateur j	f_j	$E_j(eV)$	$\Gamma_j(eV)$
1	0.65	1.9001	0.040
2	0.25	1.9315	0.050
3	1.2	2.0516	0.080
4	5	2.3065	0.8
5	12	2.4	1
6	24	2.87	0.35

It is well known in the field of plasmonics that periodicity of the plated gold nanowires would significantly influence the optical signature. Thus, our first concern was about to tune absorption for several periodicities with values ranging from 50 to 90 nm in order to understand the influence of periodicity p on the plasmonic resonance. Figure 2 a displays the obtained results in which the best value is noticed to be optimum around $p = 50$ nm.

To further study the influence of the structure's geometry, it is also important to investigate the effects on changing the pitch period p. It is worth noting that the localized effect could be observed through the absorption spectrum for the light with TM modes. Effectively, as the particle distance was decreased, the optical resonance of the structure becomes significantly strong in the light interaction; when the period of the particle array (p) was 50 nm, a strong optical absorption of light energy (77%) was shown. The absorption enhancement due to the periodicity is varying from 42% ($p = 90$ nm) to 77% ($p = 50$ nm). When the distance between the particles becomes smaller, the mutual influence of particles reveals a stronger electric field coupling effect. Thus, this fact results in an electric field enhancement that can be explained by the fact that the excited electric field is generated by the double interactions through the incident field and the resonance between nanowires. This underlying physics explains our choice of the parameter $p = 50$ nm. Let us now mention that when p varies from 50 to 90 nm, the resonant wavelength decreases and shifts to step to the blue range. These results are confirmed with experimental works in the literature for the same systems [30]. It should be noted that for a weaker coupling regime between metallic nanostructures with a larger value of particle period p, the change of p value would not have any effects on the plasmonic resonance of the particles. Therefore, within the limits of an experimental realization, the small

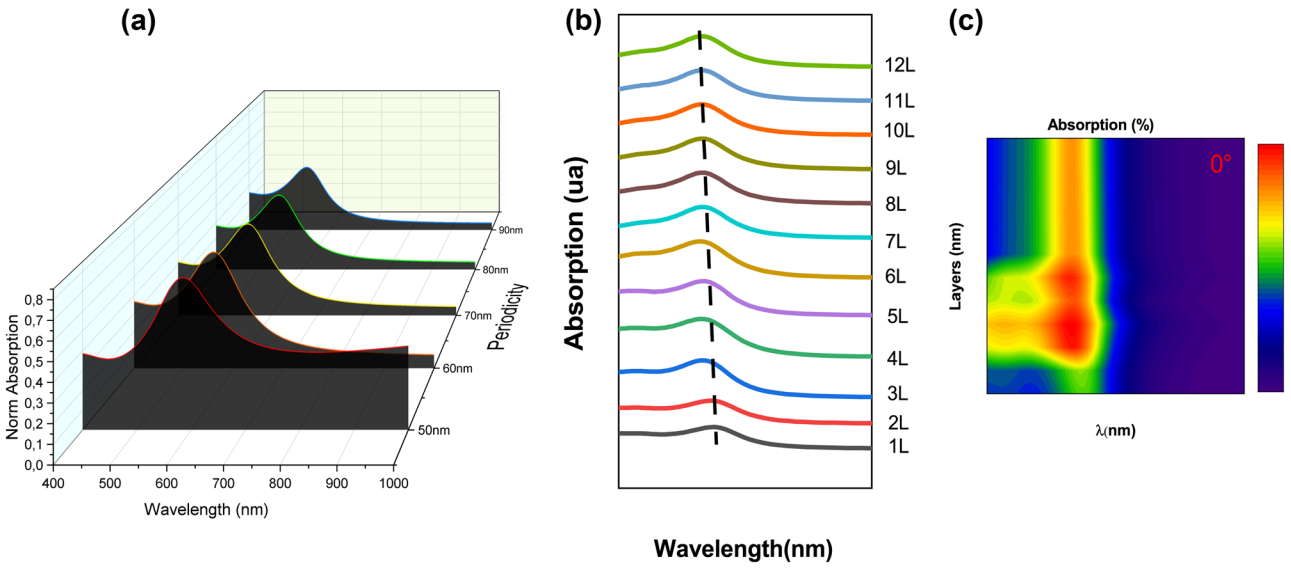

Fig. 2 **(a)** Evolution of the absorption coefficient of hexagonal gold nanowires along with period p without MoS_2 layers. **(b)** Absorption spectrum of the studied structure for several MoS_2 layers. **(c)** Color map of absorption as function of the wavelength (x-axis) and the layers (y-axis), illuminated by TM polarization for normal incident case

value of p allows this plasmonic structure concentrate and absorbs the light in the sub-wavelength volumes, which are of great interest for plasmonic solar cells. Compared with the gold rectangular ribbon structures, a stronger plasmonic effect can still be observed. This is due to hexagonal geometry that might support a stronger electric field localization at the edges of the Au NPs that are more flexible and easier to be excited in our structure compared with rectangular ribbons.

Based on the results in Fig. 2a, it can be seen that periodicity has an impact on the absorption in which we performed an enhancement from 42 to 77%. Now, we added the potential MoS_2 2D material as a spacer between glass and nanowires as they are promising materials in plasmonics. We plot the evolution of the absorption spectra with varying number of MoS_2 layers at normal incidence (Fig. 2b). Thus, we can see a blue shift of 31.5 nm between 1 and 12L. As shown in Fig. 2c, the maximum absorption is observed between 3 and 6L. For 3L of MoS_2, the absorption coefficient can reach 94.95% at 537.8 nm to 98.2% at 527.7 nm for 4L. We can notice that the optical absorption of the overall structure for the given wavelength region is significantly improved as function of MoS_2 layers.

After that, we also studied the dependence of the optical absorption for the designed MoS_2-based hexagonal gold nanowires on geometrical parameters p and H. The variation of the absorption for different layers of MoS_2 as function of the period p is presented on Fig. 3.

Similarly to the previous case (without 2D material: Fig. 2a), the period effect of the gold nanowires to the absorption spectra remains the same. By changing the period p from 50 to 80 nm, the absorption spectrum shifted to a shorter wavelength, and maximal absorption will decrease with increasing of the period, which is due to the fact that the coupling with LSPR arrays will low coupling between nanowires when the period increases. The red color in Fig. 3a manifests the strong absorption in the range from 3 to 6L.

Based on the observation of the above results, the maximal absorption has been remarkably decreased with period p to 98%, 81%, 70%, and 43% at 50 nm, 60 nm, 70 nm, and 80 nm, respectively.

In parallel, we investigate the dependence of the absorption according the thickness H of MoS_2-based hexagonal gold nanowires. As is well known, the LSPRs are very sensitive to changes of geometrical parameters. Figure 4 shows the effect of the thickness H of the nanowires. We noticed also an optical shift toward shorter wavelengths with an increasing H, while a decrease for the maximal absorption was observed which shows a high plasmonic sensitivity for smaller height values, especially for $H = 10$ nm. The optimal absorption value based on numerical simulations (99.6%) is observed for $H = 10$ nm

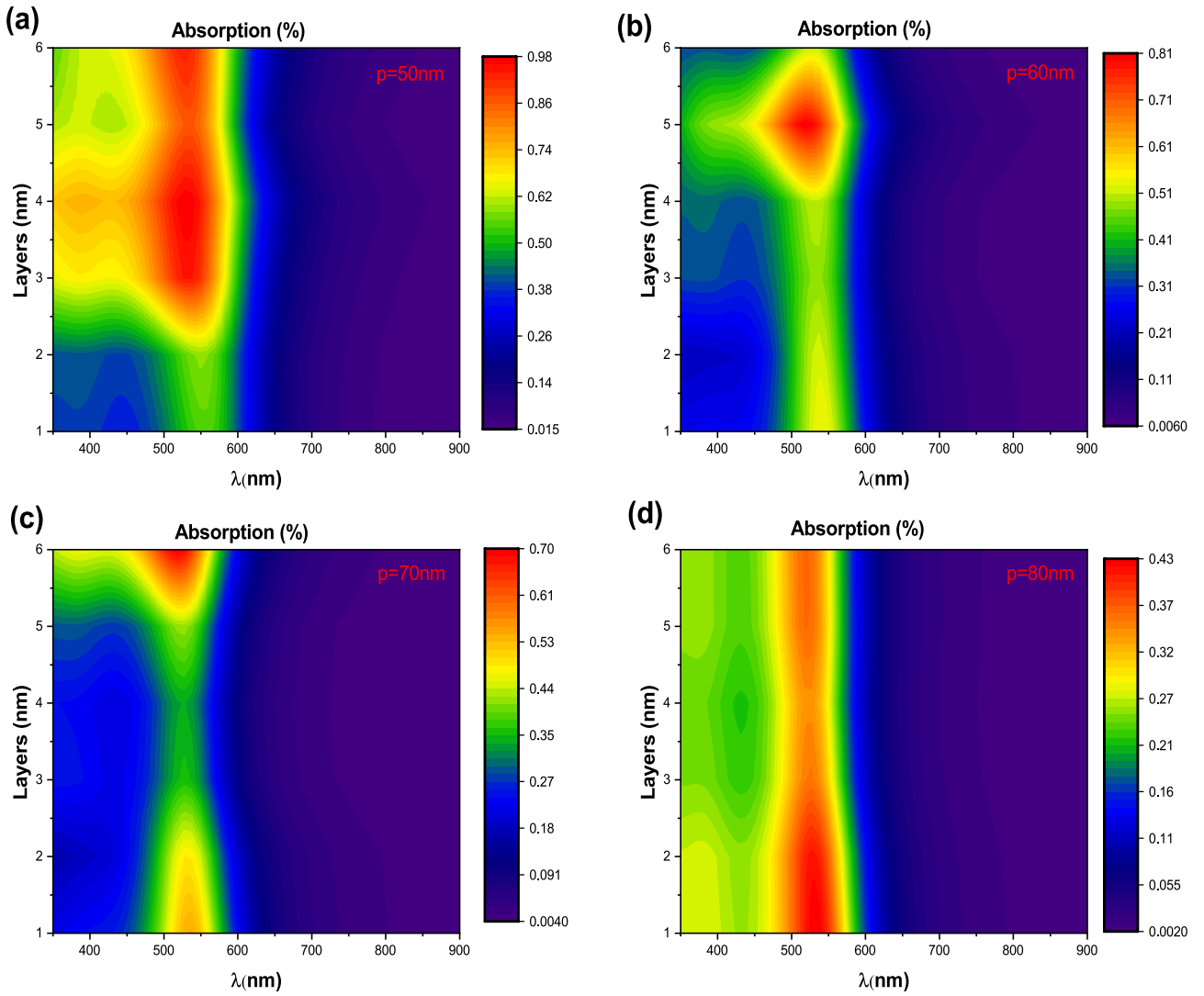

Fig. 3 Color map of absorption for different MoS_2 layers as a function of period p. (**a**) $p=50$ nm. (**b**) $p=60$ nm. (**c**) $p=70$ nm. (**d**) $p=80$ nm. The remaining geometrical parameters are held constant such as $l=30$ nm, $L=40$ nm, and $H=15$ nm

for 3L of MoS_2 at 559.24 nm (Fig. 4a). Note that the height H does not modify notably the maximal absorption, since a weak decay of 6.6% is observed in the maximal absorption when the particle height value was changed from 10 to 25 nm.

Subsequently, we have investigated the optical absorption of the MoS_2-based hexagonal gold nanowires at oblique incidence, in order to understand the effect during the presence of 2D material on the absorption enhancement. One can see in figure 5 that the maximal absorption of the proposed MoS_2-based hexagonal gold nanowires remains the same with incident angles increasing from 10° to 40° for TM polarization. Additionally, at 40°, the maximal absorption is increased for all MoS_2 layers. This fact provides both good absorption and optical stability under oblique incidence. The proposed design offers the advantage of being flexible as opposed to the showcased complicated geometries in the literature. The flexibility and simplicity of the designed structure will definitely benefit the future design of energy-harvesting nanophotonic and optoelectronic devices.

In the end, we try to provide an analysis of near-perfect absorption through the impedance transformation approach for optimal parameter value previously treated. This condition is satisfied, when the impedances of the nanowires have almost been equal to 1 (i.e., free space impedance).

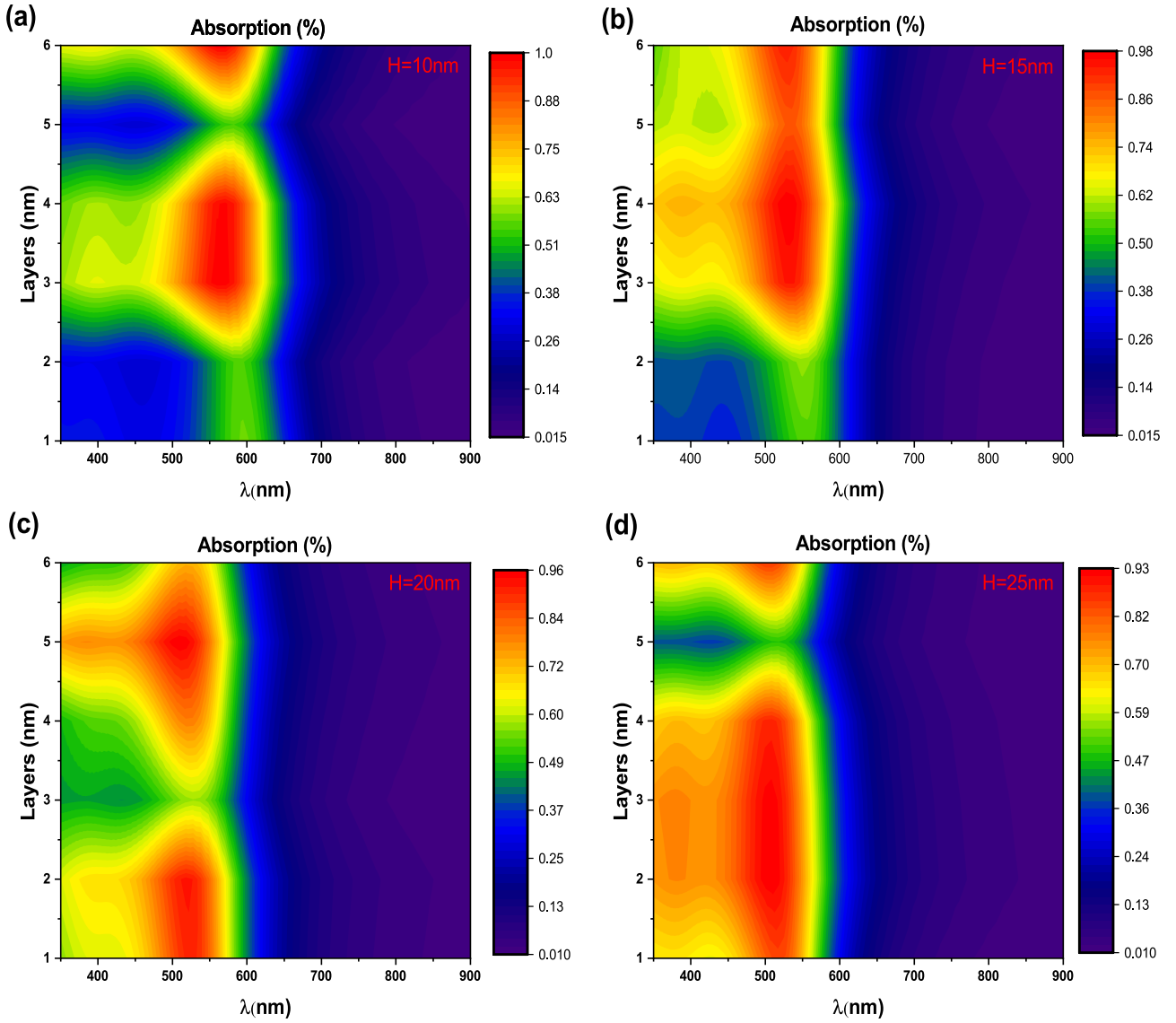

Fig. 4 Color map of absorption for different MoS_2 layers as a function of H. (**a**) $H=10$ nm. (**b**) $H=15$ nm. (**c**) $H=20$ nm. (**d**) $H=25$ nm. $l=30$ nm, $L=40$ nm, and $p=50$ nm

The blue line in Fig. 6a shows the localized SPR spectra of 3 layers of MoS_2 with the wavelengths ranging from 350 to 900 nm, and the localized SPR has been significantly improved. In order to calculate the impedance (Z), the relation between the S (S_{11} and S_{21}) parameters and Z can be easily derived with both relations [31, 32]:

$$S_{11} = \frac{i}{2}\left(\frac{1}{Z} - Z\right)\sin(nkH) \tag{1}$$

$$S_{21} = \frac{1}{\cos(nkH) - \frac{i}{2}\left(\frac{1}{Z} + \frac{1}{2}\right)\sin(nkH)} \tag{2}$$

where n, k, and H represent the effective refractive index, the electromagnetic wave vector, and the nanostructure thickness, respectively.

Therefore, the impedance is given by:

$$Z = \pm\sqrt{\frac{(1+S_{11})^2 - S_{21}^2}{(1-S_{11})^2 - S_{21}^2}} \tag{3}$$

The condition to be satisfied to achieve a near-perfect absorption is that the impedance at the resonance wavelength at working range should be near to the free-space impedance ($Z=Z_0$) [31, 32].

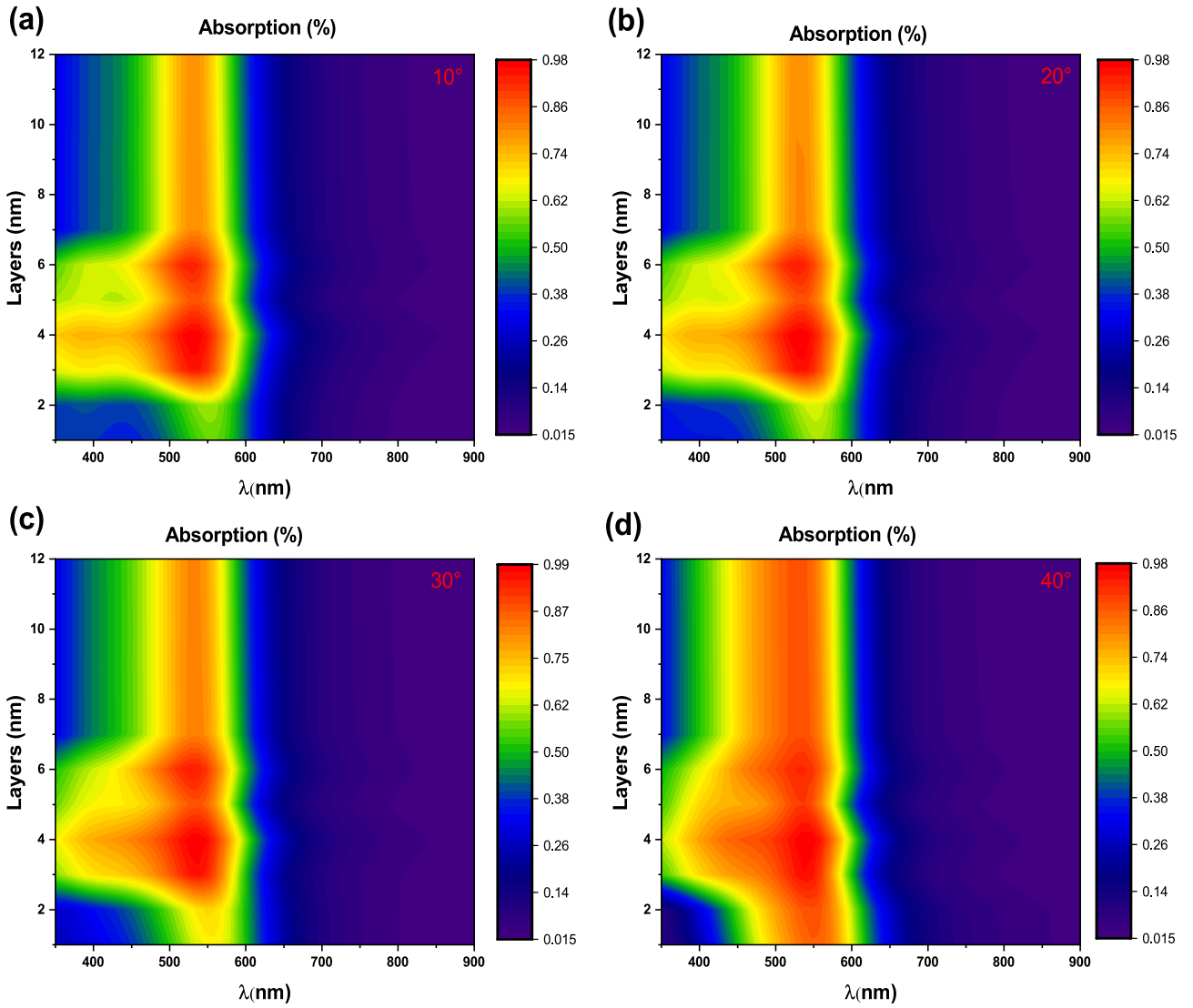

Fig. 5 Color map of absorption for different MoS_2 layers as a function of incident angle. (**a**) 10°. (**b**) 20°. (**c**) 30°. (**d**) 40°. $l = 30$ nm, $L = 40$ nm, and $p = 50$ nm

We notice at Fig. 6b that the impedance of the designed MoS_2-based hexagonal nanowires is close to 1 at the resonance wavelength of $\lambda_R = 559.24$nm, which perfectly agreed with the near-perfect absorption.

This observation is confirmed by the field maps presented in Fig. 6c, where we show the electric and magnetic field amplitude distributions at the resonance ($\lambda_R = 559.24$nm). Therefore, we can see that around the interface between hexagonal nanowires and MoS_2, the electric field and magnetic field are harvested and enhanced.

The hot spots in each of nanowire corner, and especially the two corners directly attached with TMD active layers, generally induce the losses due to the localized field intensity. In our design, the interface between gold hexagonal nanowires and the MoS_2 multilayers allows to trap and absorb light in high efficiency. This strong absorption is due to high concentration of the light energy and near-field enhancement in MoS_2 multilayers by the strong confinement through the LSPR mode located in the interface of gold nanoparticles and their corner edges.

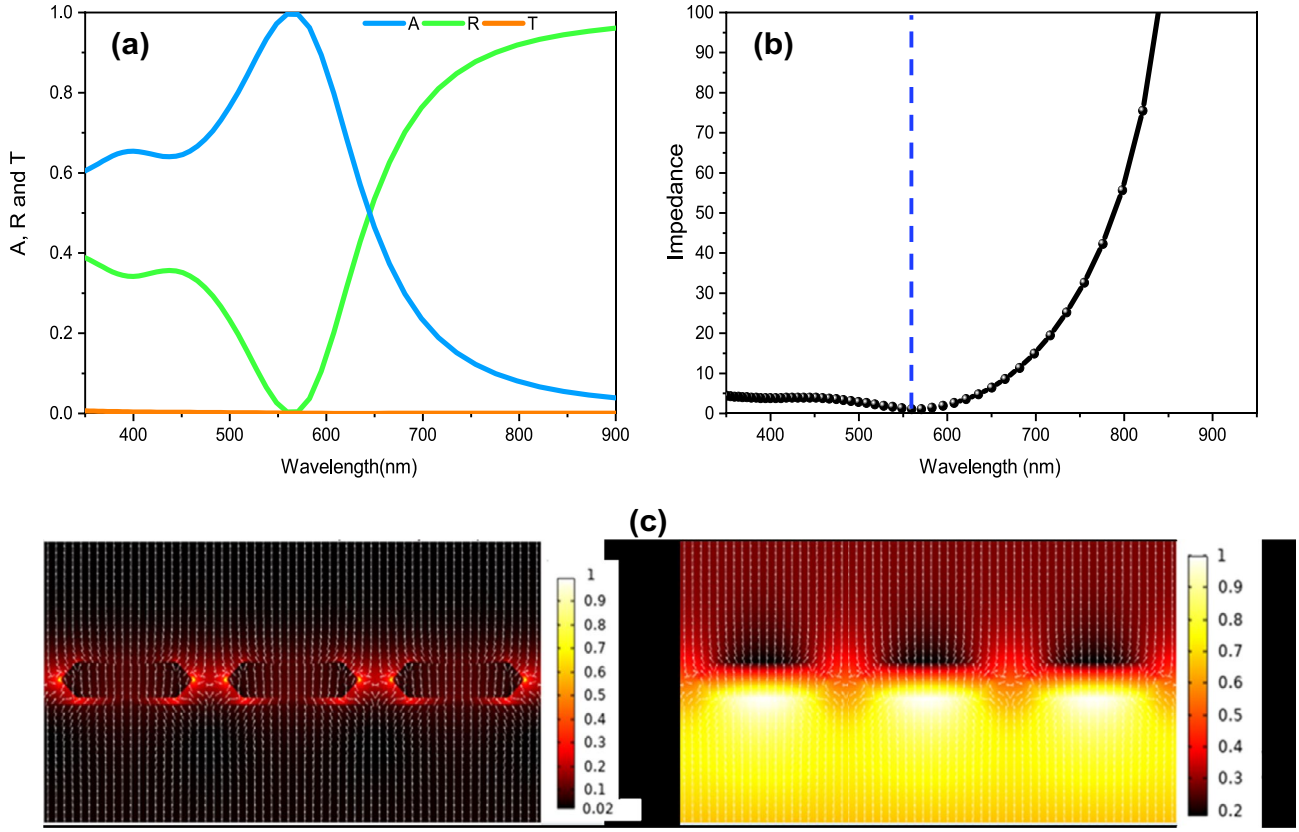

Fig. 6 **(a)** Absorption (A), reflection (R), and transmission (T) for optimal parameter (3L of MoS_2, $H=10$ nm, $p=50$ nm, $L=40$ nm, and $l=30$ nm. **(b)** Impedance of the MoS_2-based hexagonal nanowires. **(c)** The electric field $|\boldsymbol{E}|$ and magnetic field $|\boldsymbol{H}|$ amplitude distribution at resonant wavelength $\lambda_R = 559.24$nm. The white arrow is corresponding to the Poynting vector

Conclusions

In this work, a theoretical study is done to observe the effect of MoS_2 TMDs material, on the absorption coefficient and electric field distribution of a new 2D hybrid plasmonic nanostructure. The designed nanostructure is structured by a gold nanowire with hexagonal shape deposed on N layer of MoS_2 TMD material. It is demonstrated that the combined influence of MoS_2 multi-layers and gold nanowire array has significantly increased the light transmitted by the 3 layers of MoS_2, and a strong localized field concentration was achieved to enhance the optical absorption. From our results, we found that in the presence of MoS_2, the absorption of the nanostructure can reach above 99.6%. The proposed nanostructures based on the hexagonal gold nanowire with MoS_2 TMDs active layers would be a best choice for the optical nanodevices.

Acknowledgements A. Akjouj gratefully acknowledges the hospitality of the department of Physics, Faculty of Science, University of Moulay Ismail of Meknes. This work was partially supported by the program FINCOME "Centre National pour la Recherche Scientifique et Technique, Morocco".

Author contribution All calculations and writing: Z.O. Supervision of the work: A.A., A.M. Substantial contributions to the scientific discussions: S.Z, Y.A. All the authors have read and accepted the version of the manuscript.

References

1. Maier SA (2007) Plasmonics: fundamentals and applications. Springer Science & Business Media
2. Homola J, Piliarik M (2006) 'Surface plasmon resonance (SPR) sensors', in Surface plasmon resonance based sensors, J. Homola, Ed. Berlin, Heidelberg: Springer Berlin Heidelberg, pp. 45–67
3. Ouyang Q et al (2016) Sensitivity enhancement of transition metal dichalcogenides/silicon nanostructure-based surface plasmon resonance biosensor, Sci Rep, vol. 6, p. 28190, 16. https://doi.org/10.1038/srep28190
4. Zeng S et al (2020) Plasmonic metasensors based on 2D hybrid atomically thin perovskite nanomaterials, Nanomaterials, vol. 10, no. 7, Art. no. 7, Jul. https://doi.org/10.3390/nano10071289
5. Zeng S, Baillargeat D, Ho HP, Yong KT (2014) Nanomaterials enhanced surface plasmon resonance for biological and chemical sensing applications. Chem Soc Rev 43(10):3426–3452. https://doi.org/10.1039/C3CS60479A
6. Saison-Francioso O, Lévêque G, Boukherroub R, Szunerits S, Akjouj A (2015) Dependence between the refractive-index sensitivity of metallic nanoparticles and the spectral position of

their localized surface plasmon band: a numerical and analytical study. J Phys Chem C 119(51):28551–28559. https://doi.org/10.1021/acs.jpcc.5b08357
7. Galopin E et al (2010) Sensitivity of plasmonic nanostructures coated with thin oxide films for refractive index sensing: experimental and theoretical investigations. J Phys Chem C 114(27):11769–11775. https://doi.org/10.1021/jp1023839
8. Shen Y et al (2013) Plasmonic gold mushroom arrays with refractive index sensing figures of merit approaching the theoretical limit. Nat Commun 4(1):1–9. https://doi.org/10.1038/ncomms3381
9. Maurer T, Adam PM, Lévêque G (2015) Coupling between plasmonic films and nanostructures: from basics to applications. Nanophotonics 4(3):363–382. https://doi.org/10.1515/nanoph-2014-0015
10. Zeng S et al (2015) Graphene-MoS2 hybrid nanostructures enhanced surface plasmon resonance biosensors. Sens and Actuators B 207:801–810
11. Sancho-Fornes G, Avella-Oliver M, Carrascosa J, Fernandez E, Brun EM, Maquieira Á (2019) Disk-based one-dimensional photonic crystal slabs for label-free immunosensing. Biosens Bioelectron 126:315–323. https://doi.org/10.1016/j.bios.2018.11.005
12. Kelemen L, Lepera E, Horváth B, Ormos P, Osellame R, Vázquez RM (2019) Direct writing of optical microresonators in a lab-on-a-chip for label-free biosensing. Lab Chip 19(11):1985–1990. https://doi.org/10.1039/C9LC00174C
13. Oumekloul Z, Moutaouekkil M, Lévêque G, Talbi A, Mir A, Akjouj A (2020) Nanomechanical modulation cavities of localized surface plasmon resonance with elastic whispering-gallery modes. J Appl Phys 127(2):023105. https://doi.org/10.1063/1.5111819
14. Li Y et al (2016) Co-nucleus 1D/2D heterostructures with Bi2S3 nanowire and MoS2 monolayer: one-step growth and defect-induced formation mechanism. ACS Nano 10(9):8938–8946. https://doi.org/10.1021/acsnano.6b04952
15. Pillai S, Catchpole KR, Trupke T, Green MA (2007) Surface plasmon enhanced silicon solar cells. J Appl Phys 101(9):093105. https://doi.org/10.1063/1.2734885
16. Wang S et al (2019) Limits to strong coupling of excitons in multilayer WS2 with collective plasmonic resonances. ACS Photonics 6(2):286–293. https://doi.org/10.1021/acsphotonics.8b01459
17. Tsai ML et al (2014) Monolayer MoS2 heterojunction solar cells. ACS Nano 8(8):8317–8322. https://doi.org/10.1021/nn502776h
18. Cao J et al (2017) Enhanced optical absorption of monolayer WS2 using Ag nanograting and distributed Bragg reflector structures. Superlattices Microstruct 112:218–223. https://doi.org/10.1016/j.spmi.2017.09.030
19. Zhou K, Song J, Lu L, Luo Z, Cheng Q (2019) Plasmon-enhanced broadband absorption of MoS_2-based structure using Au nanoparticles. Opt Express, OE 27(3):2305–2316. https://doi.org/10.1364/OE.27.002305
20. Sun Z, Sun Z, Huang F, Fu Y (2020) MoS_2-based broadband and highly efficient solar absorbers, Appl. Opt., AO, vol. 59, no. 22, pp. 6671–6676, Aug. https://doi.org/10.1364/AO.399772
21. Lu Y et al (2018) Magnetic polariton enhanced broadband absorption and photoresponse of monolayer MoS2 based on normal and anomalous metallic gratings. J Phys D: Appl Phys 51(29):295104. https://doi.org/10.1088/1361-6463/aacab7
22. Chen M, He Y, Ye Q, Zhu J (2019) Tuning plasmonic near-perfect absorber for selective absorption applications. Plasmonics 14(6):1357–1364. https://doi.org/10.1007/s11468-019-00925-w
23. Liu J, Chen W, Zheng JC, Chen YS, Yang CF (2019) Wide-angle polarization-independent ultra-broadband absorber from visible to infrared, Nanomaterials (Basel), vol. 10, no. 1, Dec. https://doi.org/10.3390/nano10010027
24. Zhao J et al (2018) 'Light emission from plasmonic nanostructures enhanced with fluorescent nanodiamonds, Scientific Reports, vol. 8, no. 1, Art. no. 1, Feb. https://doi.org/10.1038/s41598-018-22019-z
25. Huang D et al (2015) Photoluminescence of a plasmonic molecule. ACS Nano 9(7):7072–7079. https://doi.org/10.1021/acsnano.5b01634
26. Li Y et al (2014) 'Measurement of the optical dielectric function of monolayer transition-metal dichalcogenides: MoS_2, $MoSe_2$, WS_2, and WSe_2. Phys Rev B 90(20):205422. https://doi.org/10.1103/PhysRevB.90.205422
27. Wang S et al (2016) Coherent coupling of WS2 monolayers with metallic photonic nanostructures at room temperature. Nano Lett 16(7):4368–4374. https://doi.org/10.1021/acs.nanolett.6b01475
28. Palik ED (2012) Handbook of Optical Constants of Solids.
29. Akjouj A et al (2013) Nanometal plasmonpolaritons. Surf Sci Rep 68(1):1–67. https://doi.org/10.1016/j.surfrep.2012.10.001
30. Oumekloul Z, Lahlali S, Mir A, Akjouj A (2018) Evolution of LSPR of gold nanowire chain embedded in dielectric multilayers. Opt Mater 86:343–351. https://doi.org/10.1016/j.optmat.2018.10.020
31. Smith DR, Vier DC, Koschny Th, Soukoulis CM (2005) Electromagnetic parameter retrieval from inhomogeneous metamaterials. Phys Rev E 71(3):036617. https://doi.org/10.1103/PhysRevE.71.036617
32. Wu D et al (2017) 'Numerical study of an ultra-broadband near-perfect solar absorber in the visible and near-infrared region', Opt. Lett., OL, vol. 42, no. 3, pp. 450–453, Feb. https://doi.org/10.1364/OL.42.000450